International Conference on Case Histories in Geotechnical Engineering

(1988) - Second International Conference on Case Histories in Geotechnical Engineering

02 Jun 1988, 10:30 am - 3:00 pm

The Probability of Failure of an in Stages Constructed Embankment on Soft Soil

R. J. Termaat
Ministry of Public Works, The Netherlands

E. O. F. Calle
Delft Geotechnics, The Netherlands

R. O. Petschl
Delft Geotechnics, The Netherlands

Recommended Citation

Termaat, R. J.; Calle, E. O. F.; and Petschl, R. O., "The Probability of Failure of an in Stages Constructed Embankment on Soft Soil" (1988). *International Conference on Case Histories in Geotechnical Engineering*. 53.
https://scholarsmine.mst.edu/icchge/2icchge/2icchge-session3/53

The Probability of Failure of an in Stages Constructed Embankment on Soft Soil

R.J. Termaat
Ministry of Public Works, The Netherlands

R.O. Petschl
Delft Geotechnics, The Netherlands

E.O.F. Calle
Delft Geotechnics, The Netherlands

SYNOPSIS: During construction of the first one of a twin dam in the Oosterschelde basin several instabilities occurred. Design of the construction plan of the dam was based on classical methods of analysis of stability and usually applied safety criteria. Back analysis of the failures consisted of a probabilistic analysis, indicating high overall probabilities of failure, and FEM analysis, indicating areas of large plastic deformation of the subsoil, caused by the steep setup of the sandfill in the initial construction stage, resulting in too concentrated surcharge. Based on these results, it was decided to apply these methods of analysis from the beginning in the design of the construction plan for the second dam. This plan has succesfully been carried out.

INTRODUCTION

In 1976 the Dutch government decided to build an open storm surge barrier in the Oosterschelde estuary, as final part of the Delta plan to protect the central and south west part of the Netherlands from flooding. This open barrier on the one hand will offer sufficient protection and on the other hand preserves the tidal regime in the estuary, which is desirable both from an economical and environmental point of view. Part of the plan was the construction of two separation dams, the Markiezaatskade and the Oesterdam (figure 1), in order to reduce the required number of salt intrusion and navigation locks in the economically important fairway, connecting Rotterdam and Antwerp.
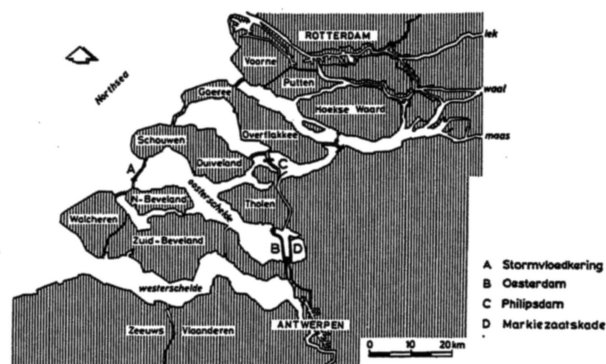

Figure 1. Situation map, south-west part of the Netherlands.

During construction of the Markiezaatskade several instabilities of the soft subsoil occurred, though usually considered factors of safety had been applied in the design of the construction plan. Post analysis has been carried out, using probabilistic analysis of stability and finite element computations to investigate the causes of failure. These

analyses indicated the following conclusions:
- The designed relatively steep slopes of the sandfill caused areas of large plastic deformation in the subsoil, leading to unexpected large settlement of the dam.
- Due to relatively concentrated surcharge relatively small failure circles have been found to be critical, the effect of which is poor averaging of variations of shear strength, resulting in fairly high probabilities of failure (order 10 %).

It was therefore decided to follow a prudent approach in the design of the Oesterdam, and it was considered useful to apply these methods of analysis right from the start in the process of developping a construction plan.

METHOD OF PROBABILISTIC STABILITY ANALYSIS

The computation model, used for probabilistic analysis of stability of the dam is based on the conceptual model discussed by Calle (1985). Basic components of this model are:
- a Gaussian homogeneous random field description of spatial fluctuations of shearing strength of the soil
- circular potential failure modes and a Bishop type of equilibrium analysis, however, adapted for second moment analysis of random variations of shearing strength.

As a consequence, the stability factor (factor of safety) F is no longer a deterministic single-le valued quantity, but instead a Gaussian random function in the along slope direction specified by its statistics: expected mean value, standard deviation and autocorrelation function. From this, estimates of the probability of occurrence of a zone where F < 1 somewhere along the slope axis and, if this occurs, an indication of the width of such zone, can be obtained.

Apart from spatial variability of shearing strength parameters, considerable uncertainty may be involved in the estimation of hydro-static and excess pore water pressures in the subsoil stratum. The sources of uncertainty

are:
- Uncertainty about the extreme phreatic level
which may occur in the course of time during
the various construction stages. Development
of the phreatic surface in the core of the
dam is strongly related with tidal fluctua-
tions and storm surge levels in the estuary
and storm durations. Critical time instants,
regarding geotechnical stability of the dam,
occur at the moment of low tide following a
high setup level during a storm. Estimates
of critical phreatic levels have been
determined, based on numerical groundwater-
flow computations and electrical conductivi-
ty analogon experiments. Combined with sta-
tistical data on the occurrence of storms,
statistical data on the occurrence of
critical phreatic levels could be derived.
The probability of geotechnical failure was
estimated as the sum of conditional probabi-
lities of failure, assuming specific phrea-
tic levels, multiplied by the probabilities
that these are extreme critical levels
during the considered time span:

$$P_f = \Sigma_i \, P_{f|h_i} \, P(h_i)$$

where P_f denotes probability of failure,
$P_{f|h_i}$ conditional probability of failure,
given critical phreatic level h_i, and $P(h_i)$
probability of h_i being the extreme level
during the considered time span.

During the construction stages due conside-
ration must be given to excess pore water
pressure development in the subsoil.
Dissipation of excess pore water pressures,
generated during the previous surcharge
steps, is expressed in terms of consolida-
tion rate factors, the factor zero denoting
an undrained situation and the factor 1.0
complete consolidation. Estimates of these
factors were based on numerical computations
of the consolidation rate. Due account for
uncertainties involved in these estimates
was given in the probabilistic analysis of
stability by considering a discrete number
of sets of consolidation rate factors,
symbolically denoted as $\{A_j\}$ and its associ-
ated probabilities of occurrence $P(A_j)$, es-
timated on the basis of empirical data ob-
tained during previous projects. The proba-
bility of failure may then be expressed as:

$$P_f = \Sigma_j \, P_{f|A_j} \, P(A_j)$$

or, in the case of uncertainty about the
extreme phreatic level:

$$P_f = \Sigma_i \Sigma_j \, P_{f|hi,A_j} \, P(A_j) \, P(h_i)$$

RESULTS OF ANALYSES OF MARKIEZAATSKADE

During the construction of the Markiezaatsdam
failures occured when the crest level was rais-
ed up to MSL + 2.00 m. The geometry shortly
before failure is given in fig. 2a. The dam
failed by subsidence of the crest, whilst the
adjacent sill slightly rose. Before failure

cracks developed at the surface of the sand
sill, which widened after the failure. The
cracks were parallel to the length axis of the
dam. About 4 or 5 days after the first insta-
bility a dark strip of blue soft clay could be
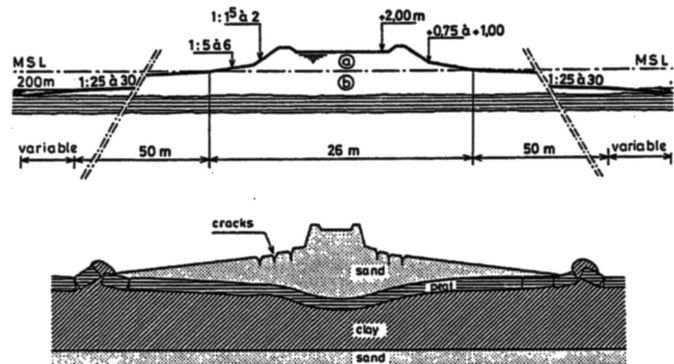seen on the edge of the sand sill (fig. 2b).

Figure 2. a. Designed cross section of the
Markiezaatskade
b. Observed deformations

The observed failures have been analysed apply-
ing a probabilistic stability approach and an
elasto-plastic FEM analysis of deformations,
i.e. the PLAXIS code (De Borst & Vermeer,
1984). The geometry and water levels applied in
the calculations are given in figure 3. The
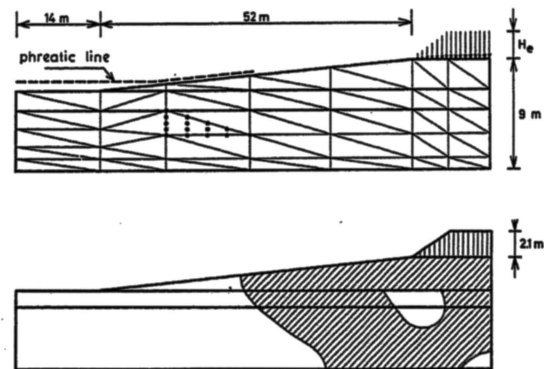soil properties are summarized in table I.

Figure 3. a. Geometry applied in probabilistic
stability and FEM analyses

b. Plastic zone found in FEM analysis

Field observations indicated failure by large
plastic deformation, resulting in settlement
rates of the crest equal to or exceeding the
surcharge rates. This could be reconstructed in
the FEM calculations, provided that the shear
modulus was adequately assessed. A good fit has
been found for G = 40 Cu (fig. 4), Cu being the
undrained shear strength, which corresponds
very well with literature data (fig. 5)

534

TABLE I. Soil parameters Markiezaatskade

depth m+MSL	soil type	γ	ϕ' μ	σ	c' μ	σ	A μ	σ
-2.55								
	peat	10	23	2.3	14	1.8	10	5
-4.10								
	organic clay	15	21	2.2	4	0.5	45	2.5
-8.60								
	sand	20	30	2.9	0	-	100	-

γ = unit weight (kN/m³)
ϕ'= angle of internal friction (°)
c'= cohesion (kN/m²)
A = consolidation rate (%)
Plasticity index organic clay: 88 ± 22 %

Statistical parameters:
μ = expected mean value
σ = standard deviation
Correlation parameters D_h= 50 m, D_v= 1 m,

assumed autocorrelation model for shear strength variations:

$$\rho(\Delta x, \Delta z) = \exp(-\Delta x^2/D_h^2 - \Delta z^2/D_v^2)$$

Δx being horizontal and Δz vertical lag

In the design an overall factor of safety against stability (Bishop analysis) of 1.15 had been applied, which is fairly low, but considered acceptable because:
- it was within our scope of experiences
- the strength data were based on Dutch cell tests and are generally conservative because in the test procedure limited the deformation rates are applied (Heynen & van Duren, 1979)
- we considered a construction stage in which slight failure would cause only limited damage.
The zone with critical slip circles corresponds with the plastic zone, found in the FEM analysis (Termaat et al, 1985)
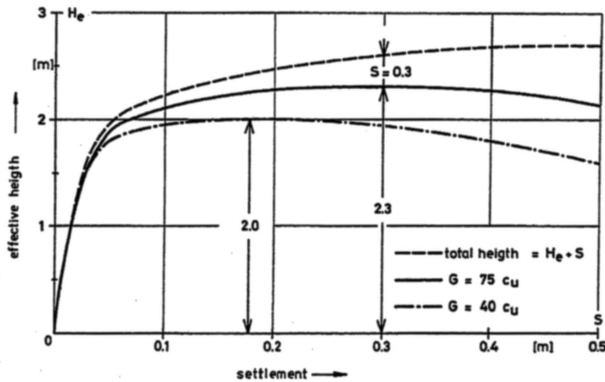
Figure 4. Effective surcharge height vs settlement

The probabilistic stability analyses resulted in a probability of failure of 0.08, which is fairly high. The main reason for it being the small perimeter of the critical slip circle, resulting in poor averaging of strength variations.
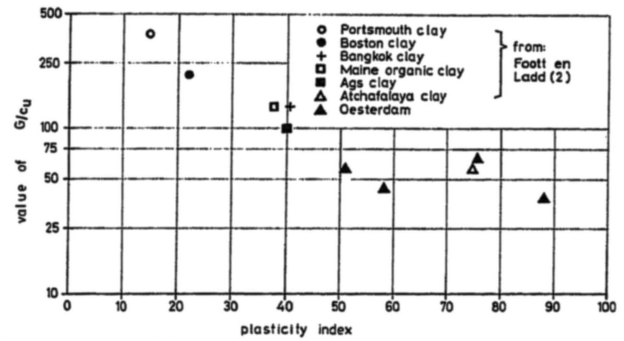
Figure 5. G/Cu ratio vs plasticity index

CONSTRUCTION PLAN FOR THE OESTERDAM

A three stage construction plan has been designed, roughly as indicated in figure 6. The stages will be referred to as the hydraulic sanfill stage (0-50 days), the intermediate preloading or consolidation stage (50-230 days) and the stage of final completion.
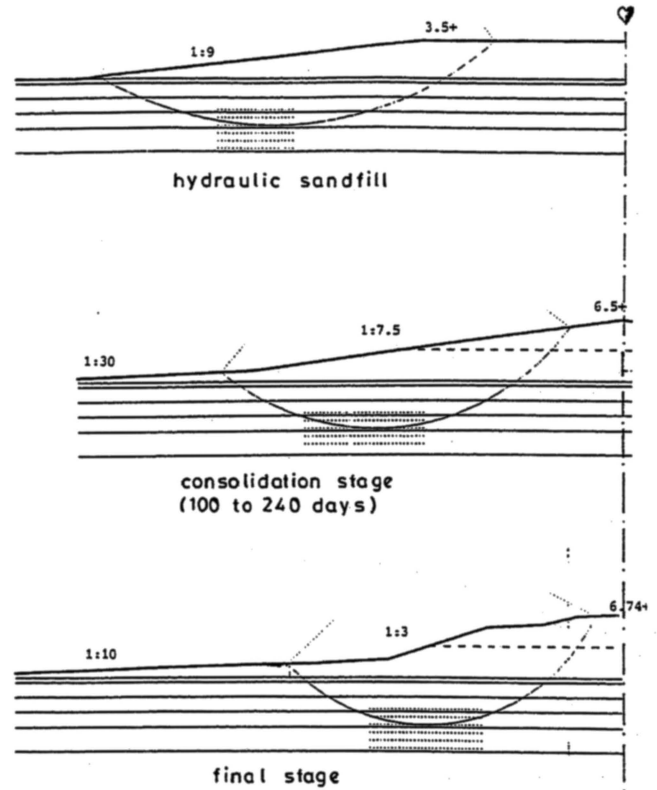
Figure 6. Envisaged construction stages of Oesterdam

The second stage, preloading during nearly one year, was planned to obtain both a sufficient reduction of the deformations and an adequate increase of stability. For each stage the probability of failure was determined with a probabilistic stability analysis for the characteristic section C2 of the dam (fig. 7). Based on this probabilistic approach safety factors for each stage had been determined and applied in the design of the other dam sections.The possibility of failure due to large

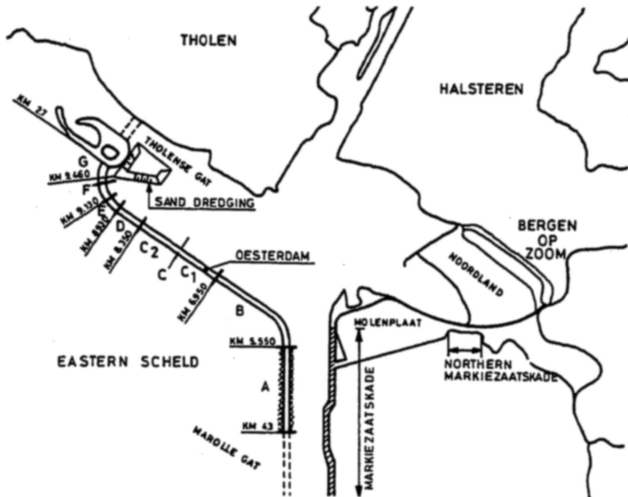plastic deformations has been checked by elasto-plastic finite element analysis.

Figure 7. Situation of dam sections

SOIL PARAMETERS OESTERDAM

A great number of borings and static cone penetration tests (CPT) have been conducted in the stretch of the Oesterdam. Undisturbed samples were taken at five locations and subjected to compression tests (Dutch cell), oedometer tests and permeability tests. At damsection C2 additional investigation has been carried out, consisting of:

- One ϕ 29 mm Begemann type boring (continuous sampling), 1.6 to 9 m below MSL.
- One CPT with the Dutch cylindrical piezo-cone, 1.6 - 13 m below MSL, measuring cone resistance and excess pore water pressures generated at a penetration rate of 20 mm/s.
- Two sensitive CPT's (sensitivity five times as normal), 1.6 to 10 m below MSL.
- Vane tests at seven levels (unremoulded and remoulded).
- Mini-pressuremeter tests.
- Laboratory testing, including determination of sample unit weight, plasticity index of clay samples, and average unit weight per meter depth, determined from the continuous samples.
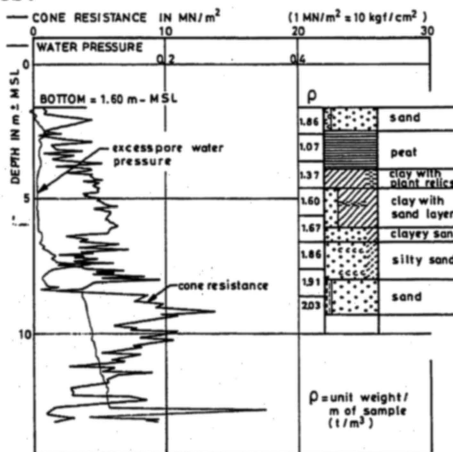

Figure 8. Results of piezo cone test and soil profile from continous sampling.

A continuous sample profile is given in figure 8, together with the piezo cone measurement results. As can been seen excess pore water pressures indicate the impermeable layers. The results of the sensitive CPT's and the unremoulded shear strenghes determined from the vane tests are given in figure 9. In the mini pressuremeter test, a ϕ 22 mm cell, mounted on a tube is pushed into the soil. The cell membrane consists of overlapping strips. The elastic shear modulus (G) of the soil is derived from the soil's reaction to volume increase of the cell. The results are summarized in table II. The average cone resistances have been included in this table for comparison.
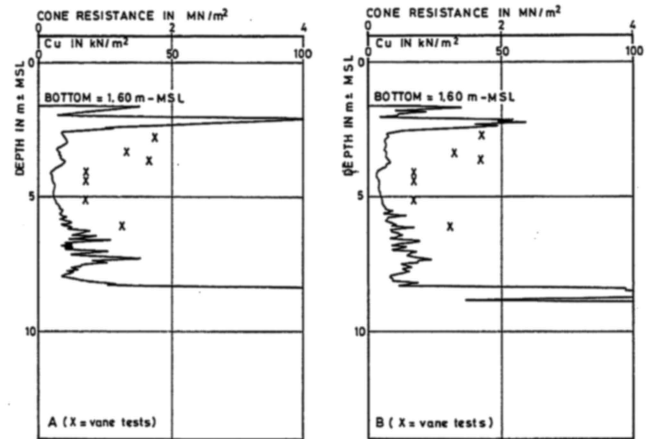

Figure 9. Results of sensitive CPT's and vane tests

TABLE II. Cone resistance and elastic shear modulus.

depth	soil type	average cone resistance	G
m - MSL		kN/m²	kN/m²
2.8	peat	300	550
3.4	peat	250	378
3.7	peat	300	484
4.1	organic clay	150	436
4.4	organic clay	200	392
5.1	silty clay + org. mat.	200	313
6.1	sandy clay	400	716

In the field vane tests only the unremoulded undrained shear strength was considered. Following Bjerrum (1972), the undrained shear strength has been reduced as function of the index of plasticity (figure 10). Unit weight (γ), water content (WC), index of plasticity (PI) and results of vane tests (Cu), with and without reduction have been given in table III.
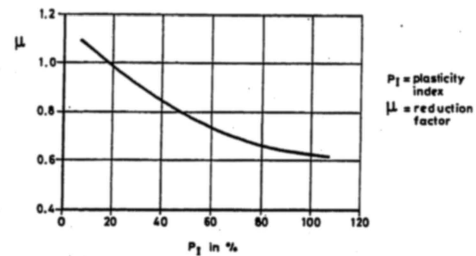

Figure 10. Reduction of undrained shear strength

TABLE III. Undrained shear strength

Depth m - NAP	γ kN/m³	PI %	WC %	Cu kN/m²	μ	Cu x μ kN/m²
2.8	10.7		59	44		
3.35	10.5		53	33		
3.7	10.8		51	42		
4.1	14.3	76	96	17	.7	12
4.4	15.9	52	78	17	.8	14
5.1	16.5	38	60	17	.9	15
6	18.4	-	37	31		

The mean values for cohesion and angle of internal friction, as used in the stability analyses, are based on approximately 10 cell tests for each soil type. The standard deviations have been assessed on the basis of observed scatter in the test results and intuition. The values have been summarized in table IV. Results of the oedometer test are included in this table.

TABLE IV. Soil parameters used in the probabilistic stability analysis (sec. C2).

top of layer	γ_s	μ_c'	μ_φ'	σ_c'	σ_φ'	C_p	C_s
1.5m-MSL	20	0	33	0	3.3		
2.5	20	0	30	0	3	100	800
3.4	10	12.8	28	2.6	5.6	4	51
4.3	10.5					5	46
5.7	13.5	2	23	0.2	2.3	8	77
6.5	18.9					83	663
11.0	17.7	2.4	24	0.2	2.4	26	439
13.2	19.3					79	301

γ_s = submerged unit weight (kN/m³)

$\mu_{c'}$, $\mu_{\phi'}$ mean value of cohesion, friction angle

$\sigma_{c'}$, $\sigma_{\phi'}$ standard deviations

C_p, C_s compression constants

Autocorrelation parameters as indicated in table I.

CRITICAL PHREATIC LEVELS, HYDRAULIC CONDITIONS

An important aspect of the analysis of stability of the dam concerns assessment of the phreatic water table in the dam. This level is highly influenced by tidal fluctuations and set up due to storms. Due to phreatic storage and limited draining capacity the water table response to tidal fluctuations involves phase

shift, causing high phreatic levels at the critical time instants, i.e. at low tide in the estuary. Estimates of the critical phreatic levels have been determined on the basis of numerical calculations and experiments with an electrical conductivity analogon. In table V the determined phreatic levels as function of the corresponding high tide levels have been summarized. The probabilities of occurrence of these high tide levels have been indicated in this table. They have been derived from high tide level frequencies as observed during a number of years (figure 11) and extrapolation of the observed frequency curve. Note that the

probabilities of occurrence of the correspon ding critical phreatic levels do not exactly coincide with the probabilities of occurrence of high tide levels. This has been done to take into account to effects, namely:
- Uncertainty involved in the determination of the phreatic level corresponding to some high tide level, which would cause the probability of occurrence of high phreatic levels to be underestimated.
- In many cases, the low tide level, following a storm, will still be influenced by the storm setup and not reach the normal low tide level. As a consequence the probability of occurrence of the combination of high phreatic level and normal low tide level would be overestimated.
The procedure to take these effects into account is as follows. The probability associated with some critical phreatic level is calculated as the weighed mean of the probabilities of occurrence of the corresponding high tide level, the next higher one and the next lower one, applying weight factors of 0.5, 0.25 and 0.25 respectively.

TABLE V. Water levels and probabilities

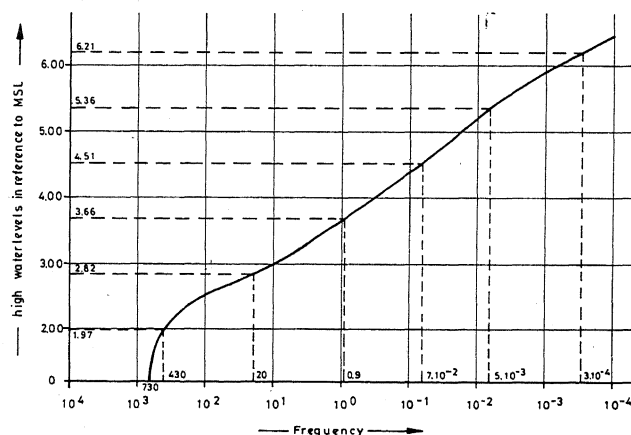| High tide level (including storm setup)		Corresponding critical phreatic level	
level	probability	level	probability
	4.3 10⁻⁷		2.1 10⁻⁶
6.21+MSL		4.03+MSL	
	7.0 10⁻⁶		2.6 10⁻⁵
5.36		3.48	
	8.9 10⁻⁵		3.5 10⁻⁴
4.51		2.93	
	1.1 10⁻³		7.1 10⁻³
3.66		2.38	
	2.6 10⁻²		1.5 10⁻¹
2.82		1.83	
	5.6 10⁻¹		3.9 10⁻¹
1.97		1.28	
	4.1 10⁻¹		4.5 10⁻¹

Figure 11. Observed frequencies of high tides

The hydraulic conditions applied in the stability analysis, can be summarized as follows. During the hydraulic sandfill stage normal low tide level and completely saturated sandfill. During the consolidation stage and after completion of the dam normal low tide level and critical phreatic levels.

EXCESS PORE WATER PRESSURES

Dissipation of excess pore water pressures, induced by surcharging in the various construction stages, has been calculated on the basis of 1-D consolidation analysis. The governing soil properties are compression coefficients as function of effective soil stress (figure 12a) and permeability as function of effective soil stress (figure 12b).
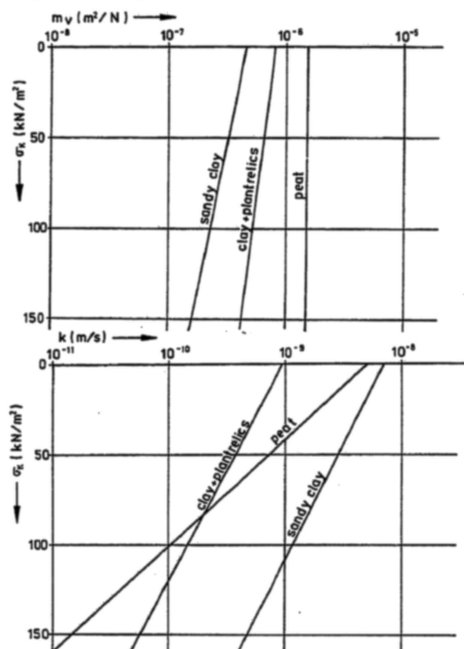

Figure 12. (a) Compression coefficients (m_v)
(b) Permeability (k)

The results of the consolidation analyses, expressed in terms of expected consolidation rates, are summarized in table VI. Estimated standard deviations have been included.

TABLE VI. Expected consolidation rates and estimated standard deviations.

stage:	sandfill	preloading	final
top sandfill (m + MSL):	3.5	6.5	6.0
slope :	1:9	1:7.5	≈1:4
consolidation rates (%):			
peat	15 (5)	30 (8)	40 (10)
org. clay	3 (3)	10 (3)	20 (5)
sandy clay	3 (3)	10 (3)	30 (8)
sand + clay	5 (5)	25 (6)	55 (14)

Parenthesized values indicate standard deviations.
Predicted hydrodynamic period of preloading stage is 0.5 year.

The indicated consolidation rates reflect expected subsoil adaption at the start of each of the construction stages.

CALCULATED PROBABILITIES OF FAILURE

Computations have been carried out for the sandfill and preloading stages and for three subsequent periods of 100 days after completion of the dam. Results of computations for the hydraulic fill stage are summarized in table VII. As mentioned previously complete saturation has been assumed, so only uncertainty concerning the consolidation rates is involved. Weighed summation of conditional probabilities yields an estimate of the probability of failure in this stage of $5 \cdot 10^{-3}$. The expected failure width equals 20 - 30 m.

TABLE VII. Results of probabilistic computations for the hydraulic fill stage (Section C2).

A_i	F	$P_{f|A_i}$	$P(A_i)$	L
$\mu - 2\sigma$		$3 \cdot 10^{-2}$*	0.066	
$\mu - \sigma$	1.15	$8 \cdot 10^{-3}$	0.243	27 m
μ	1.18	$1.5 \cdot 10^{-3}$	0.382	23 m
$\mu + \sigma$	1.21	$3 \cdot 10^{-4}$	0.309	21 m

μ : expected consolidation rate
σ : standard deviation of consolidation rate
F : expected mean factor of safety
$P_{f|A_i}$: conditional probability
$P(A_i)$: probability of consolidation rate A_i
L : expected failure width

* extrapolated value

The results of computations for the consolidation stage are summarized in table VIII. In this stage both consolidation rate and extreme phreatic level are considered uncertain. The conditional probabilities, given a specific phreatic level in table VIII, have been determined accounting for uncertainty of consolidation rates similar to the procedure applied for the hydraulic fill stage. The intermediate results however have been omitted for reasons of space limitation. Weighed summation of failure probabilities yields an estimate of the probability of failure of $8 \cdot 10^{-5}$ during the consolidation stage.

TABLE VIII. Probabilities of failure during the consolidation stage (Section C2).

h_p	F	$P_{f|h_p}$	$P(h_p)$	L
3.75 + MSL	1.19	$2.5 \cdot 10^{-3}$	0.001	20-35 m
3.20	1.24	$1.5 \cdot 10^{-4}$	0.015	20-30 m
2.65	1.29	$1.4 \cdot 10^{-6}$	0.813	15-20 m
2.10	1.34	$1.4 \cdot 10^{-7}$	0.023	10-15 m
1.55	1.40	$< 10^{-7}$	-	10-15 m

TABLE VIII. Continued

---

h_p = phreatic level (m + MSL).

$P(f|h_p)$ = Conditional probability of failure.

$P(h_p)$ = Prob. that h_p is the extreme level during the considered timespan.

F   = Expected mean of factor of safety.

Similar computations have been carried out for the final stage, after completion of the dam. Three subsequent periods of 100 days have been analyzed. The intermediate results of the computation are omitted, the final results are given in table IX.

Table IX. Probabilities of failure after completion of the dam (section C2).

Period	F	P_f	L
0 - 100 days	1.20	$5 \cdot 10^{-2}$	
100 - 200 days	1.27	$5 \cdot 10^{-3}$	30 - 100 m
200 - 300 days	1.30	$4 \cdot 10^{-4}$	

OBSERVED CONSOLIDATION RATES AND SETTLEMENTS

At five locations in the stretch of the dam Kistler type piezometers and settlement gauges have been installed, to monitor excess pore pressure dissipation and settlement. In the pilot section C2 seven piezometers, measuring pore water pressures in the sandfill, the deep sand and in the cohesive layers. Results of these measurements are plotted in figure 13.
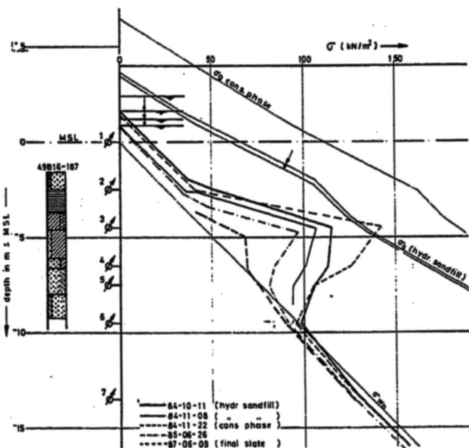

Figure 13. Observed pore water pressures in dam section 2.

From these measurements the consolidation rates have been determined, as indicated in figure 14. It is concluded that the dissipation rates were much greater than expected, and that the envisaged consolidation stage of 130 days was substantially more than actually required.

The settlements have also been measured and compared to the expected settlements, revealing a similar tendency, however no indication has

been found that the final settlements will substantially differ from the predicted ones.
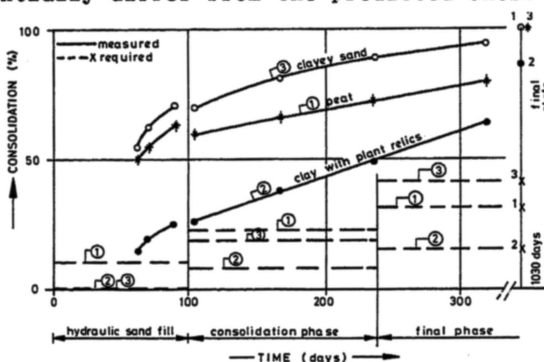

Figure 13. Observed consolidation rates.

The observed rapid development of excess pore pressure dissipation indicates that consolidation rates have been considerably underestimated. The actual consolidation rates even exceed the optimistic ($\mu + \sigma$) levels. Based on this observation the following (posterior) adjustments of the probabilities of failure could be made: for the consolidation stage $P(f) < 10^{-6}$ and for the first 100 day period after completion $P(f) < 3 \cdot 10^{-5}$, based on the conditional probabilities of failure assuming ($\mu + \sigma$) consolidation rates.

PLASTIC DEFORMATIONS

Figure 14 shows the development of zones of plastic shear when applying ultimate loading. Computed crest settlements versus surcharge are shown in figure 15, revealing an ultimate surcharge height of 7 m. The actually applied surcharge height was 4.5 m.

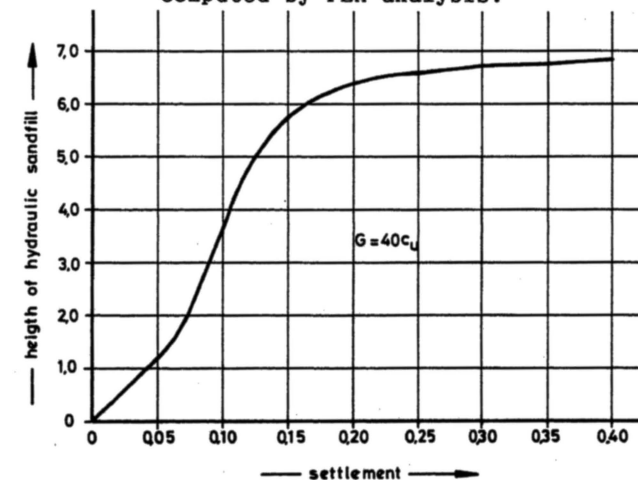Figure 14. Zones of plastic shear as computed by FEM analysis.

Figure 15. Height of sandfill vs settlement.

OVERALL SAFETY FACTORS

The computed prior probabilities of failure
were considered acceptable, at least as far as
the first and second construction stage are
concerned. Hence, the use of corresponding
factors of safety was considered acceptable in
the design for the other sections of the dam,
since no substantially different subsoil
strength and dissipation behaviour was ex-
pected. The applied factors of safety were 1.15
for the hydraulic fill stage and 1.20 for the
consolidation stage.

CONCLUSIONS

- Steep setup of the sandfill of the Markie-
  zaatskade is considere the main cause of
  failure due to plastic deformation. This
  mechanism was found much less relevant for
  the Oesterdam, because of the flat slopes of
  the sandfill envisaged in the design.
- Identical factors of safety, applied in the
  design of both Markiezaatskade and Oesterdam,
  led to substantially different probabilities
  of failure. The reason for it being the smal-
  ler slip circle, in case of the Markiezaats-
  kade, leading to poor averaging og strength
  variation and thus a high probability of
  failure.
- Based on the observed high consolidation
  rates, it would have been possible to reduce
  the envisaged preloading period. This adjust-
  ment of the design has not been considered.
- In the construction of embankments on soft
  soil with high plasticity index, attention
  should be paid to large plastic deformation.
- The factor of safety, as determined in
  classical stability analysis, is less
  decisive regarding safety as is generally
  assumed.

ACKNOWLEDGEMENT

REFERENCES

Bjerrum, L. (1972), "Embankments on soft
  Ground", Proceedings of Speciality Conference
  of Earth and Earth Supported Structures,
  Volume III.
Borst, R. de & P.A. Vermeer (1984), "Possibili-
  ties and Limitations of Finite Elements for
  Limit Analysis", Geotechnique 34, no. 2.
Calle, E.O.F. (1985), "Probabilistic analysis
  of stability of earth slopes", Proc. XIth
  ICSFME, San Francisco.
Heynen, W.J. & F.J. van Duren (1979), "The
  Dutch Cell Test, Comparison of Results of
  Cell Tests and Triaxial Tests on Clay", Proc.
  VIIth ECSMFE, Brighton U.K., volume 2.
Termaat, R.J., P.A. Vermeer & G. Vergeer
  (1985), "Failure by large plastic deforma-
  tions", Proc. XIth ICSMFE, San Francisco.